PAPER

Check for updates

Semi-enzymatic synthesis and application of ^{13}C-isotopically labelled inositol-(1,4,5)-trisphosphate†

Atharva Patharkar, [iD] [ab] Meike Amma, [iD] [ab] Jaime Isern,[a] Zoé Chaudron,[c] Angélique Besson-Bard,[c] Valérie Nicolas-Francès,[c] Claire Rosnoblet,[c] David Wendehenne,[c] Peter Schmieder [iD] [a] and Dorothea Fiedler [iD] *[ab]

Inositol-(1,4,5)-trisphosphate (Ins(1,4,5)P$_3$) is a crucial secondary messenger that controls calcium (Ca^{2+}) levels inside cells, yet many questions regarding Ins(1,4,5)P$_3$ metabolism are challenging to address with current methods. Here, a semi-enzymatic milligram scale synthesis of isotopically labeled [^{13}C$_6$]Ins(1,4,5)P$_3$ is reported which then served as a substrate to monitor the activity of mammalian type II inositol 1,4,5-trisphosphate 5-phosphatase INPP5B, using NMR spectroscopy in real time. In addition, the phosphorylation sequence catalyzed by inositol polyphosphate multikinase IPMK was confirmed using [^{13}C$_6$]Ins(1,4,5)P$_3$ and 2D NMR spectroscopy. The method was subsequently applied to characterize the phosphorylation/dephosphorylation reactions of a putative inositol phosphate kinase from the alga *Klebsormidium nitens* (*Kn*IPK2). *Kn*IPK2 displayed 6-kinase activity towards [^{13}C$_6$]Ins(1,4,5)P$_3$, and dual 4/6- and 5-phosphatase activity towards [^{13}C$_6$]Ins(1,3,4,5,6)P$_5$. Finally, [^{13}C$_6$]Ins(1,4,5)P$_3$ was utilized as an internal standard in hydrophilic liquid interaction chromatography mass spectrometry (HILIC-MS) experiments, to quantify dephosphorylation of Ins(1,4,5)P$_3$ by INPP5B. [^{13}C$_6$]Ins(1,4,5)P$_3$ therefore constitutes a broadly applicable analytical tool that should facilitate the characterization of Ins(1,4,5)P$_3$ metabolism in the future.

Introduction

Inositol-(1,4,5)-trisphosphate (Ins(1,4,5)P$_3$) is a secondary messenger critically involved in the regulation of calcium (Ca^{2+}) release within mammalian cells.[1] The formation of Ins(1,4,5)P$_3$ is triggered by activation of phospholipase C, which hydrolyses phosphatidylinositol 4,5-bisphosphate (PtdInsP$_2$) and releases Ins(1,4,5)P$_3$ from the membrane. Ins(1,4,5)P$_3$ binds to its receptors on the endoplasmic reticulum and induces Ca^{2+} release into the cytosol, which mediates a variety of cellular responses.[1,2] In mammals, the level of soluble Ins(1,4,5)P$_3$ is regulated by different kinases and phosphatases. Inositol polyphosphate multikinase (IPMK) converts Ins(1,4,5)P$_3$ *via* two consecutive phosphorylation reactions to Ins(1,3,4,5,6)P$_5$.[3,4] The Ins(1,4,5)P$_3$ levels are also maintained through dephosphorylation by different classes of phosphatases. For instance, position 5 of the Ins(1,4,5)P$_3$ scaffold is dephosphorylated by

dedicated phosphatases, such as inositol polyphosphate 5-phosphatase (5-phosphatases).[5,6] The product of the latter can be further dephosphorylated by other position-specific phosphatases such as inositol polyphosphate 4-phosphatase (INPP4A) and inositol polyphosphate 1-phosphatase (INPP1) which dephosphorylate positions 4 and 1 of the InsP scaffold, respectively.[7–10]

Imbalances in mammalian inositol phosphate (InsP) metabolism have been associated with numerous detrimental cellular outcomes.[11] Inhibition of the InsP kinases IPMK and inositol 1,3,4-trisphosphate 5/6-kinase 1 (ITPK1) has been linked with blockage of necroptosis.[12] Mutations in multiple inositol polyphosphate phosphatase (MINPP1) result in intracellular accumulation of Ins(1,2,3,4,5,6)P$_6$, which leads to pontocerebellar hypoplasia involving basal ganglia.[13,14] In order to get a deeper understanding of the underlying biochemical processes in case of such disorders, it is important to develop tools that directly report on the activity and specificity of InsP kinases and phosphatases.

Classically, kinase activity is often assessed using commercially available kits that monitor ATP depletion, while radiolabeled substrates combined with high-performance liquid chromatography (HPLC) and inositol phosphate standards allow precise determination of phosphorylation sites.[3,15] However, these approaches typically require non-physiological

[a] *Leibniz-Forschungsinstitut für Molekulare Pharmakologie (FMP), Robert-Rössle-Str. 10, 13125 Berlin, Germany. E-mail: fiedler@fmp-berlin.de*

[b] *Institut für Chemie, Humboldt-Universität zu Berlin, Brook-Taylor-Str. 2, 12489 Berlin, Germany*

[c] *Université Bourgogne Europe, Institut Agro Dijon, INRAE, UMR Agroécologie, 17 rue Sully, 21065 Dijon cedex, France*

† Electronic supplementary information (ESI) available. See DOI: https://doi.org/10.1039/d5cb00139k

ATP concentrations[16,17] or availability of facilities to handle radioactivity. Similarly, phosphatase activity can be tracked by measuring the release of inorganic phosphate from the substrate, providing an indirect readout of substrate conversion.[15,18] In the case of $Ins(1,4,5)P_3$, kinase assays may not fully capture its phosphorylation dynamics and phosphatase assays do not provide conclusive insights into its dephosphorylation sequence. Therefore, deducing how $Ins(1,4,5)P_3$ is directly processed by its respective enzymes still remains a challenge.

Our group has developed strategies to synthesize ^{13}C-labeled *myo*-inositol and ^{13}C-labeled inositol polyphosphates and utilized them in metabolic labeling and biochemical experiments, in combination with nuclear magnetic resonance (NMR) spectroscopy.[19,20] Conversion of the labeled inositol phosphates can be followed directly, and in real time, using NMR.[21] Additionally, the latter method provides critical structural information on the precise position of the phosphoryl groups on the inositol ring.[20,22] The utility of this approach was demonstrated by deciphering the complex dephosphorylation sequences of MINPP1, a human phytase-like enzyme.[22] Interestingly, Jessen and coworkers recently utilised a bacterial phytase to synthesise $Ins(1,2,3)P_3$ from $Ins(1,2,3,4,5,6)P_6$.[23]

We now extend the toolset of ^{13}C-labeled inositol phosphates to include [13]C_6-labeled $Ins(1,4,5)P_3$. In this study, we have utilized MINPP1, an inositol phosphate phosphatase, to generate $[^{13}C_6]Ins(1,4,5)P_3$ from the substrate $[^{13}C_6]Ins(1,3,4,5,6)P_5$ on milligram scale. $[^{13}C_6]Ins(1,4,5)P_3$ was subsequently used as a substrate for two well-characterized $Ins(1,4,5)P_3$-metabolizing enzymes: the human type II inositol 1,4,5-trisphosphate 5-phosphatase (INPP5B) and the human kinase IPMK. Additionally, we characterized the activity of a putative inositol polyphosphate multikinase from the green algae *Klebsormidium nitens* (*Kn*IPK2), which also displayed unexpected ATP-synthase activity. Finally, we applied the labeled compound as a mass-spectrometry (MS) standard, thereby showcasing the broad applicability of $[^{13}C_6]Ins(1,4,5)P_3$ for investigating $Ins(1,4,5)P_3$-metabolism in complex systems.

Results and discussion

Semi-enzymatic synthesis of $[^{13}C_6]Ins(1,4,5)P_3$

Given the central role of $Ins(1,4,5)P_3$ in inositol phosphate signaling, we planned to obtain $[^{13}C_6]Ins(1,4,5)P_3$ to use it as a biochemical tool. Previously, Lämmerhofer *et al.* have isolated $Ins(1,4,5)P_3$ on a nanogram scale by supplying cells with ^{13}C inositol and subsequently isolating inositol phosphates.[24] The observation that MINPP1 catalyzed dephosphorylation of $Ins(1,3,4,5,6)P_5$ led to formation of $Ins(1,4,5)P_3$ as an intermediate, motivated us to exploit this reactivity.[22] We therefore sought to scale up the enzymatic conversion of $[^{13}C_6]Ins(1,3,4,5,6)P_5$ to $[^{13}C_6]Ins(1,4,5)P_3$ (Fig. 1(A)).

To obtain milligram quantities of $[^{13}C_6]Ins(1,4,5)P_3$, $[^{13}C_6]Ins(1,3,4,5,6)P_5$ was synthesized according to the previously published procedure.[20] Next, 175 μM of $[^{13}C_6]Ins(1,3,4,5,6)P_5$ were treated with 0.5 μM MINPP1 in HEPES buffer at 37 °C for 4 h. The reaction was followed using NMR spectroscopy. We found that the
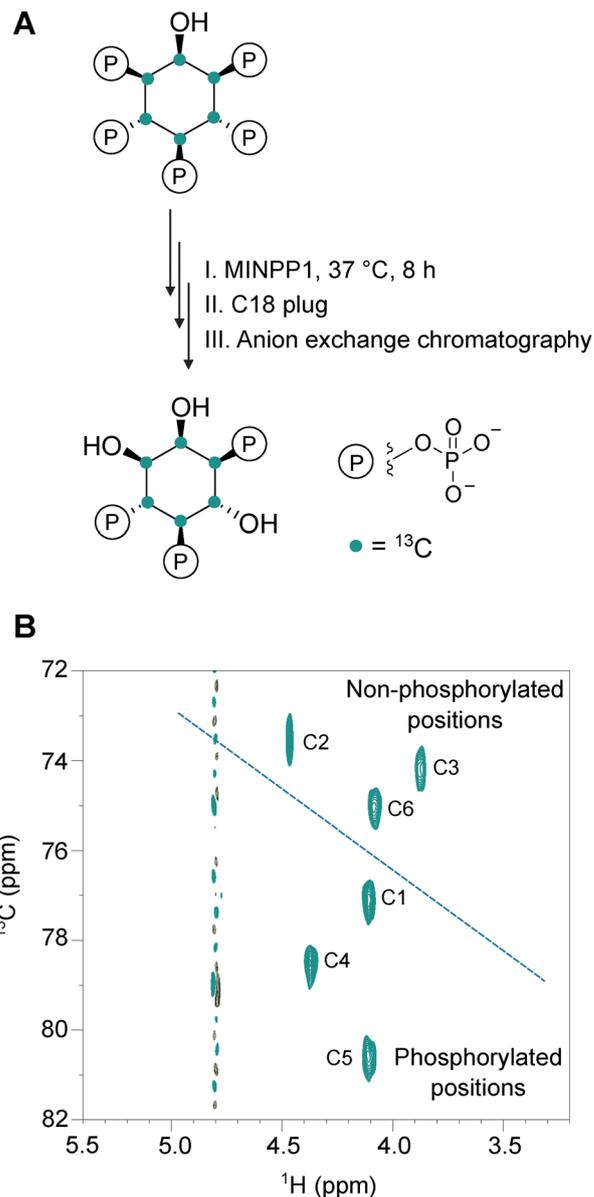
Fig. 1 (A) Generation of labeled $[^{13}C_6]Ins(1,4,5)P_3$ using MINPP1 and $[^{13}C_6]Ins(1,3,4,5,6)P_5$. The reaction was carried out at 37 °C in H_2O for 8 h with 175 μM substrate and 0.5 μM MINPP1. (B) Assignment of carbon positions of $[^{13}C_6]Ins(1,4,5)P_3$ in $^1H–^{13}C$ HMQC NMR spectrum. The separation of the region for non-phosphorylated *versus* phosphorylated positions is indicated by a dotted line.

increased reaction volume appeared to slow down the conversion, compared to our previous report,[22] and therefore we extended the reaction time. When 175 μM $[^{13}C_6]Ins(1,3,4,5,6)P_5$ were incubated with 0.5 μM MINPP1 for 8 h at 37 °C, the majority of the product was $[^{13}C_6]Ins(1,4,5)P_3$. After heat quenching the reaction, the mixture was subjected to strong anion exchange chromatography using an ammonium bicarbonate gradient to separate the remaining inositol phosphate species. The fractions were analysed using NMR and fractions containing $[^{13}C_6]Ins(1,4,5)P_3$ were then lyophilized to provide $[^{13}C_6]Ins(1,4,5)P_3$ as a white powder in high yield (70%).

© 2025 The Author(s). Published by the Royal Society of Chemistry

RSC Chem. Biol., 2025, **6**, 1426–1436 | **1427**

In order to confirm the nature of the product, we utilised ^{1}H–^{13}C HMQC NMR spectroscopy. A ^{1}H–^{13}C HMQC NMR spectrum can identify cross-correlations between ^{13}C nuclei and the protons that are directly attached to them. The ^{1}H–^{13}C HMQC NMR spectrum confirmed the isolation of the desired product when compared with the chemical shifts reported by Trung et al.[22] Compared to the starting material, the dephosphorylation of positions 3 and 6 was corroborated by the upfield shift of the corresponding ^{1}H chemical shifts from 4.10 ppm to 3.83 ppm for position 3, and from 4.08 ppm to 4.05 ppm for position 6 (Fig. 1(B)). In contrast, the remaining phosphorylated positions (1, 4, and 5) displayed characteristic downfield shifts in the ^{1}H–^{13}C HMQC NMR spectrum, consistent with previous literature.[22] The non-phosphorylated atoms C2 (^{1}H: 4.39 ppm, ^{13}C: 73.54 ppm), C3 (^{1}H: 3.83 ppm, ^{13}C: 74.07 ppm), and C6 (^{1}H: 4.05 ppm, ^{13}C: 75.12 ppm) were clearly separated from the phosphorylated atoms C1 (^{1}H: 4.10 ppm, ^{13}C: 76.74 ppm), C4 (^{1}H: 4.33 ppm, ^{13}C: 78.39 ppm), and C5 (^{1}H: 4.08 ppm, ^{13}C: 80.25 ppm) (Fig. 1(B)).

[^{13}C$_6$]Ins(1,4,5)P$_3$ as a substrate to directly measure INPP5B 5-phosphatase activity

To validate [^{13}C$_6$]Ins(1,4,5)P$_3$ as a biochemical tool, we monitored the dephosphorylation activity of mammalian INPP5B, a well characterised 5-phosphatase with similar activities towards PtdIns(4,5)P$_2$ and Ins(1,4,5)P$_3$.[25] 200 μM [^{13}C$_6$]Ins(1,4,5)P$_3$ were incubated with 20 nM INPP5B at 30 °C for 30 min and the reaction mixture was heat quenched, diluted, and subsequently analyzed by ^{1}H–^{13}C HMQC NMR spectroscopy (Fig. 2(A)).[25]

We anticipated the formation of Ins(1,4)P$_2$, based on numerous previous reports.[25–28] For optimal spectral resolution and chemical shift dispersion, we recorded a ^{1}H–^{13}C HMQC spectrum. The ^{1}H–^{13}C HMQC spectrum unambiguously demonstrated that INPP5B converts Ins(1,4,5)P$_3$ to Ins(1,4)P$_2$. The resonance of Ins(1,4,5)P$_3$ (^{1}H: 4.08 ppm, ^{13}C: 80.25 ppm) corresponding to the C–H at position 5 begins to disappear upon treatment with INPP5B and a new, upfield shifted resonance was detected at (^{1}H: 3.64 ppm, ^{13}C: 77.12 ppm), for the C–H at the corresponding dephosphorylated position of Ins(1,4)P$_2$ (Fig. 2(B)). This direct visualization confirmed that the synthesized [^{13}C$_6$]Ins(1,4,5)P$_3$ serves as an effective probe to monitor specific dephosphorylation events. While it was known that the reaction product would be Ins(1,4)P$_2$, the systematic analysis of changes in the NMR chemical shifts will also enable the assignment of new, unanticipated reaction products, for which the relevant standards may not be available.

Based on the notable chemical shift change at position 5 upon dephosphorylation by INPP5B, real time monitoring of INPP5B phosphatase activity on Ins(1,4,5)P$_3$ appeared feasible. The 1D proton signals of the inositol phosphates are in close proximity to those of the buffer and water, making it difficult to follow the reaction conversion. However, the ^{1}H–^{13}C HMQC NMR spectrum provided clear peak separation between Ins(1,4,5)P$_3$ and Ins(1,4)P$_2$ at position 5, enabling their differentiation. By limiting the spectral width in the ^{13}C dimension, and by stacking HMQC spectra recorded at different time points, the dephosphorylation of Ins(1,4,5)P$_3$ by INPP5B could
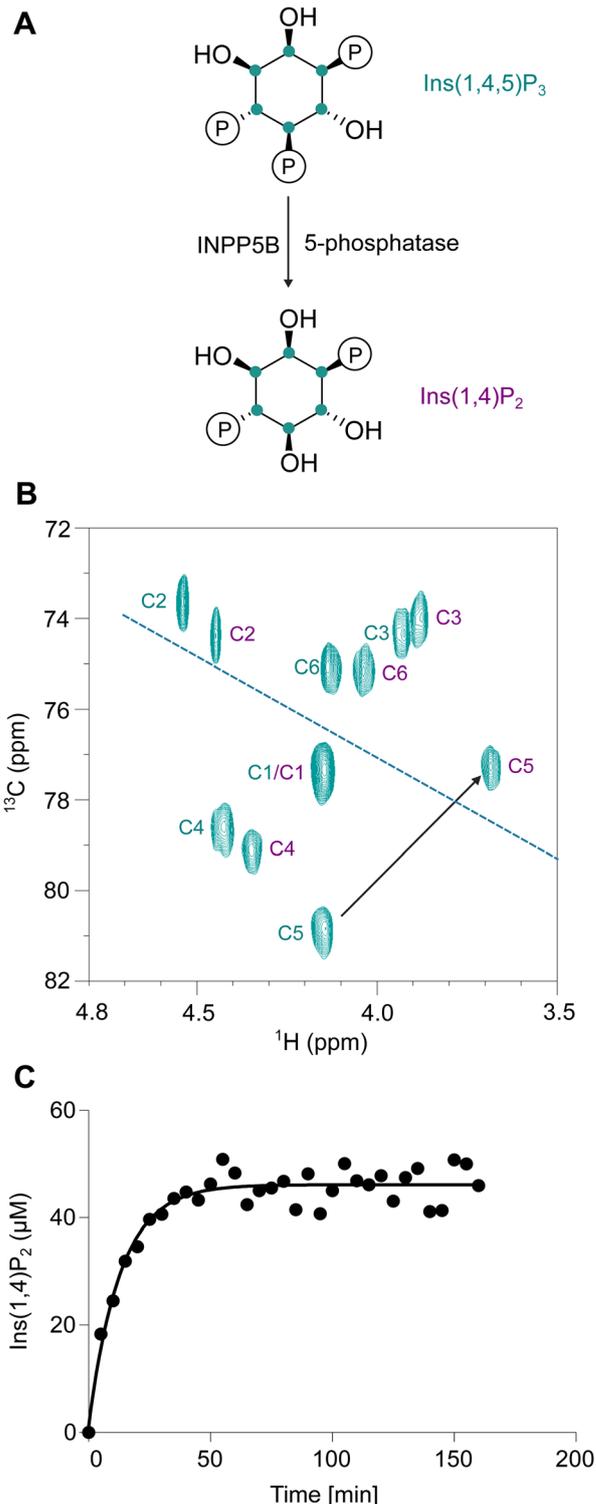

Fig. 2 (A) Dephosphorylation of Ins(1,4,5)P$_3$ by INPP5B. (B) ^{1}H–^{13}C HMQC NMR spectrum of a reaction mixture in which 200 μM [^{13}C$_6$]Ins(1,4,5)P$_3$ was treated with 20 nM INPP5B at 30 °C for 30 min. The reaction mixture contains both Ins(1,4)P$_2$ and Ins(1,4,5)P$_3$, as indicated by the teal and purple labels, respectively. The signal for position 5 undergoes a diagnostic shift. The separation of the region for non-phosphorylated versus phosphorylated positions is indicated by a dotted line. (C) NMR based real-time monitoring of INPP5B phosphatase activity by exploiting 5′-non-phosphorylated position of Ins(1,4)P$_2$. 50 μM substrate was incubated with 10 nM INPP5B. 33 HMQC spectra were recorded at intervals of 3 min 49 seconds. The graph represents the appearance of position 5 of Ins(1,4)P$_2$ against time.

be monitored in real-time. 10 nM INPP5B was added to 50 μM Ins(1,4,5)P$_3$ in the reaction buffer in D$_2$O, and 33 ^{1}H–^{13}C HMQC NMR spectra were recorded at the time intervals of 3 min 49 seconds. The peak intensity of the appearing Ins(1,4)P$_2$ position 5 over time was transformed into molarity and was plotted against time (Fig. 2(C)). Based on the consumption of Ins(1,4,5)P$_3$, the initial rate for INPP5B was calculated to be 9.60 μmol mg^{-1} min^{-1}.

[^{13}C$_6$]Ins(1,4,5)P$_3$ as a substrate to directly measure kinase activity

We then investigated if [^{13}C$_6$]Ins(1,4,5)P$_3$ can be used to monitor a phosphorylation sequence using the IPMK. IPMK is an evolutionarily conserved enzyme known to have a dual 3-kinase and 6-kinase activity. Human IPMK converts Ins(1,4,5)P$_3$ to Ins(1,3,4,5)P$_4$ followed by conversion to Ins(1,3,4,5,6)P$_5$ (Fig. 3(A)).[29,30] So far, the activity of IPMK could only be monitored by HPLC using radiolabelled inositol phosphate species and has relied on the availability of the respective standards.[29,30]

To probe the activity of IPMK, 175 μM [^{13}C$_6$]Ins(1,4,5)P$_3$ was incubated overnight with 300 nM IPMK and 2 mM ATP at 37 °C. The reaction mixture was directly analyzed by recording a ^{1}H–^{13}C HMQC NMR spectrum. Based on the absence of Ins(1,4,5)P$_3$ signals, we concluded 100% conversion of the substrate after overnight incubation and two major inositol phosphate species were present in the sample; a more abundant asymmetrical species, and a less abundant symmetrical compound (Fig. 3(B)). The asymmetrical species appeared to be phosphorylated at the position 3, as indicated by a downfield shift in both the ^{1}H and ^{13}C dimensions (Fig. 3(B)). Comparison to a standard reference (Fig. S1, ESI†) identified the more abundant species as Ins(1,3,4,5)P$_4$. The less abundant, symmetrical compound (Fig. 3(B)) was subsequently assigned as Ins(1,3,4,5,6)P$_5$, using chemically synthesized [^{13}C$_6$]Ins(1,3,4,5,6)P$_5$ as the reference.[20] The formation of Ins(1,3,4,5)P$_4$ and Ins(1,3,4,5,6)P$_5$ from Ins(1,4,5)P$_3$ is consistent with literature reports that have used radiolabelled Ins(1,4,5)P$_3$ as substrate.[29]

Characterization of the activity of microalgal inositol polyphosphate kinase (*Kn*IPK2)

Following the validation with the known enzymes INPP5B and IPMK, we tested [^{13}C$_6$]Ins(1,4,5)P$_3$ as tool to investigate a putative inositol polyphosphate kinase. *Kn*IPK2 from the green alga *Klebsormidium nitens* has 37.2% sequence identity with *At*IPK2α, a well characterized inositol polyphosphate kinase from *Arabidopsis thaliana* (Fig. S2, ESI†).[31,32] *At*IPK2α phosphorylates Ins(1,4,5)P$_3$ to Ins(1,3,4,5,6)P$_5$ using ATP as phosphate donor.[33,34] We wondered if *Kn*IPK2 displays a similar activity and employed [^{13}C$_6$]Ins(1,4,5)P$_3$ as tool to investigate this question.

We expressed *Kn*IPK2 in *E. coli* (Fig. S3, ESI†) and incubated 200 μM [^{13}C$_6$]Ins(1,4,5)P$_3$ with 20 nM of the enzyme at 37 °C and 2 mM ATP in presence of 10 mM MgCl$_2$ at pH 7.7. After incubation for 6 h, the formation of a new inositol phosphate species was observed (Fig. 4(A)). The signal for the position 6 of Ins(1,4,5)P$_3$ began to disappear, while a downfield-shifted signal of a putative phosphorylated species appeared, indicating that
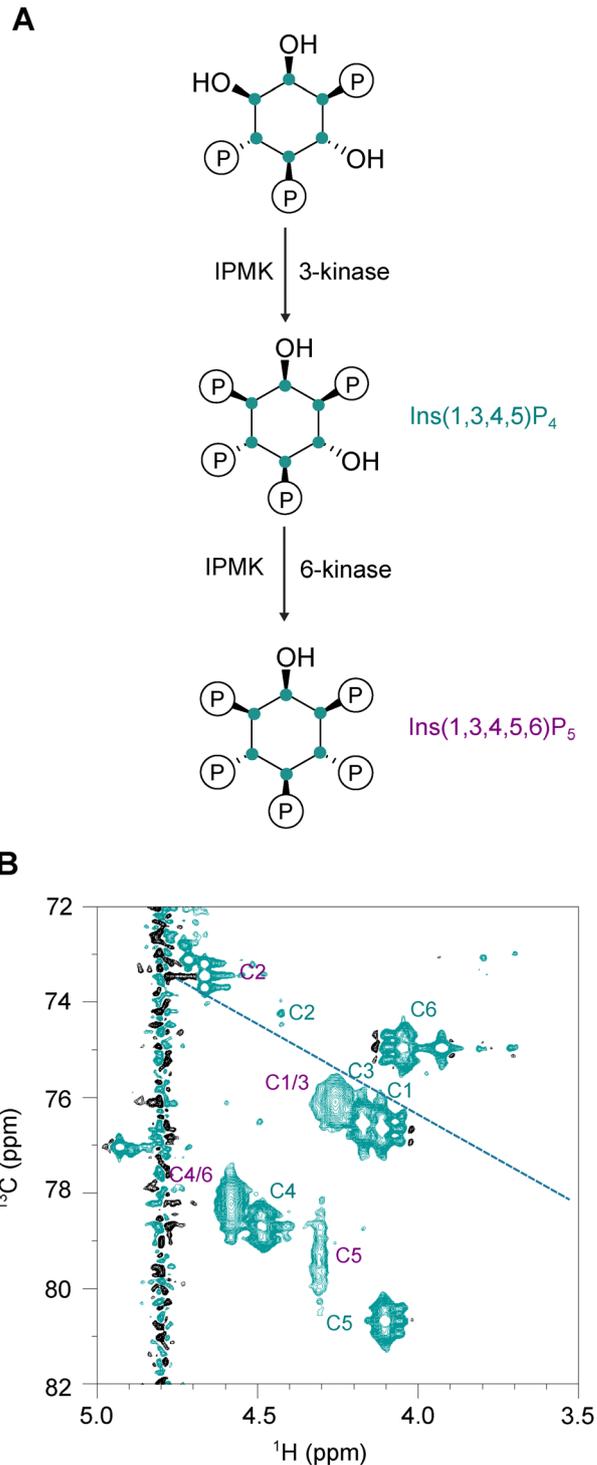
Fig. 3 (A) IPMK catalyzed phosphorylation of Ins(1,4,5)P$_3$. (B) ^{1}H–^{13}C HMQC NMR spectrum of a reaction mixture in which 175 μM [^{13}C$_6$]Ins-(1,4,5)P$_3$ was treated with 300 nM IPMK overnight. The reaction products were assigned as Ins(1,3,4,5)P$_4$ (teal) or Ins(1,3,4,5,6)P$_5$ (purple). The separation of the region for non-phosphorylated *versus* phosphorylated positions is indicated by a dotted line.

*Kn*IPK2 converts Ins(1,4,5)P$_3$ to Ins(1,4,5,6)P$_4$ (Fig. 4(A)). This hypothesis was confirmed using ^{1}H–^{13}C HMQC-CLIP-COSY NMR spectroscopy, a pulse sequence for detecting cross correlations
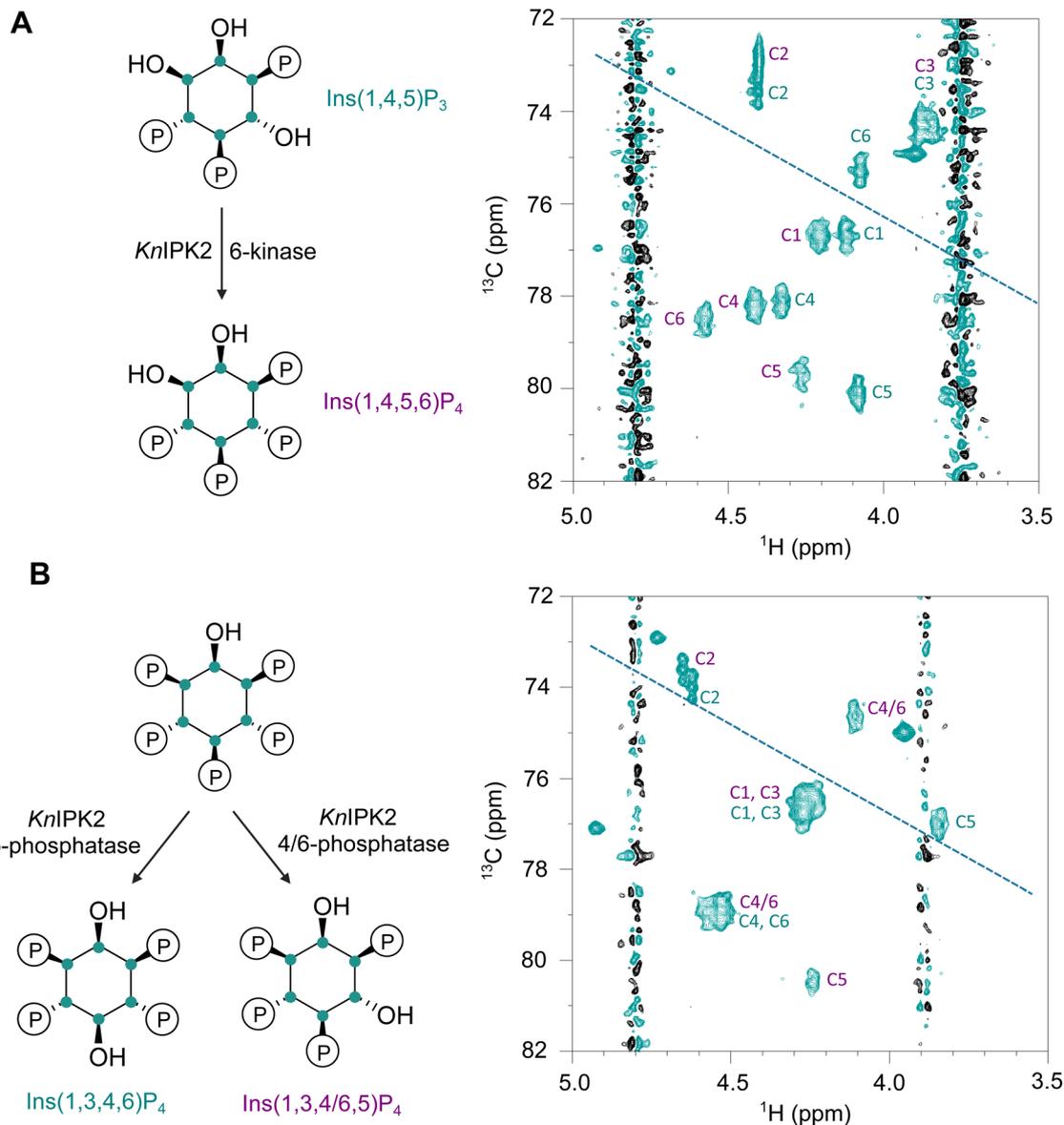
© 2025 The Author(s). Published by the Royal Society of Chemistry

RSC Chem. Biol., 2025, **6**, 1426–1436 | **1429**

Fig. 4 (A) *Kn*IPK2 catalyzed phosphorylation of Ins(1,4,5)P$_3$ (teal) to yield (1,4,5,6)P$_4$ (purple), measured by ^{1}H–^{13}C HMQC NMR spectroscopy. (B) ^{1}H–^{13}C HMQC NMR spectrum of *Kn*IPK2 catalyzed dephosphorylation of Ins(1,3,4,5,6)P$_5$ to its products Ins(1,3,4/6,5)P$_4$ (purple) and Ins(1,3,4,6)P$_4$ (teal). For both phosphorylation and dephosphorylation reactions, 200 μM substrate was incubated with 20 nM *Kn*IPK2 at 37 °C for 6 h with 2 mM ATP or ADP, respectively. The separation of the region for non-phosphorylated *versus* phosphorylated positions is indicated by a dotted line.

between two adjacent ^{1}H–^{13}C pairs. The new peak exhibited partial cross-correlation with position 1 of the InsP species (Fig. S4, ESI†). For the final identification, a ^{1}H–^{13}C HMQC spectrum of Ins(1,4,5,6)P$_4$ was recorded and the identity of the kinase reaction product was confirmed to be Ins(1,4,5,6)P$_4$ (Fig. S5, ESI†). Unlike its plant ortholog *At*IPK2α, *Kn*IPK2 could not further phosphorylate Ins(1,4,5,6)P$_4$ into Ins(1,3,4,5,6)P$_5$ using longer incubation times, elevated ATP concentrations (from 250 μM to 2 mM) or introducing an ATP recycling system.[33]

We next explored the potential dephosphorylation activity of *Kn*IPK2. After incubation of 20 nM *Kn*IPK2 with 200 μM Ins(1,3,4,5,6)P$_5$ and 2 mM ADP, the ^{1}H–^{13}C HMQC spectrum revealed two distinct species. one compound that was

dephosphorylated at position 5, and one compound, which was dephosphorylated either at position 4 or 6 (Fig. 4(B)). We recorded a ^{1}H–^{13}C HMQC-CLIP-COSY NMR spectrum, which confirmed dephosphorylation at position 5, identifying one compound as Ins(1,3,4,6)P$_4$ (Fig. S6 and S7, ESI†). The ^{1}H–^{13}C HMQC-CLIP-COSY NMR spectrum also revealed that the other compound was dephosphorylated either at positions 4 or 6. We assigned it as Ins(1,3,4/6,5)P$_4$ (Fig. S6, ESI†). This was further corroborated using Ins(1,3,4,5)P$_4$ as standard (Fig. S1 and S7, ESI†), however unambiguous assignment of the positions 4 or 6 was not possible. Such ambiguity may be resolved in future by using ʟ-arg-amide as a chiral solvating agent or using asymmetrically labelled InsPs as the substrates for the reaction.[22,35]

A

B
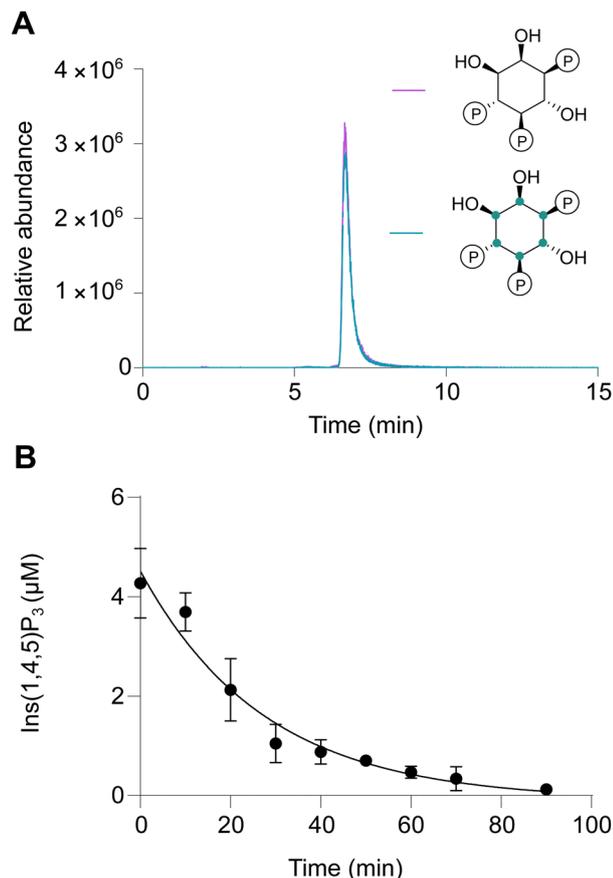
Fig. 5 (A) Elution profiles and extracted ion chromatograms of $[^{13}C_6]Ins(1,4,5)P_3$ (teal) and $[^{12}C_6]Ins(1,4,5)P_3$ (pink). The y-axis displays the relative abundance of the respective species extracted from the total ion chromatogram (TIC). (B) Time course of $Ins(1,4,5)P_3$ consumption. 50 μM $Ins(1,4,5)P_3$ was incubated with 20 nM INPP5B and the reaction was quenched at time intervals of 10 min. The samples were diluted 10-fold, $[^{13}C_6]Ins(1,4,5)P_3$ subsequently was added to the final concentration of 3.6 μM, and the mixture was analyzed by HILIC-MS.

Use of $[^{13}C_6]Ins(1,4,5)P_3$ as a standard in mass spectrometry

In addition to utilizing $[^{13}C_6]Ins(1,4,5)P_3$ in NMR spectroscopy, we envisioned another application for this tool as a mass spectrometry standard. The field of inositol phosphate metabolism has been significantly advanced since the introduction of chromatography coupled with mass spectrometry (MS).[36] We therefore aimed at using hydrophilic interaction chromatography (HILIC) coupled with MS to demonstrate the utility of $[^{13}C_6]Ins(1,4,5)P_3$ as an internal MS standard to track consumption of $[^{12}C_6]Ins(1,4,5)P_3$ by INPP5B.

To obtain quantification with accuracy independent of the ionization source, stable isotope dilution analysis was employed. First, a calibration curve of peak area for $[^{12}C_6]Ins(1,4,5)P_3/[^{13}C_6]$-$Ins(1,4,5)P_3$ ion count *vs.* the concentrations of $[^{12}C_6]Ins(1,4,5)P_3$ was generated. This standard curve exhibited an R^2 value of 0.989, and was employed to calculate the unknown concentrations of $[^{12}C_6]Ins(1,4,5)P_3$ in reaction mixtures by spiking in $[^{13}C_6]$-$Ins(1,4,5)P_3$ as an internal standard (Fig. S8, ESI†). To quantify unlabelled $Ins(1,4,5)P_3$ in a biochemical sample, we treated 50 μM

$Ins(1,4,5)P_3$ with 10 nM INPP5B and heat-inactivated the reactions at 10 min time intervals. The reaction mixtures were filtered through a 3 kDa filter, and $[^{13}C_6]Ins(1,4,5)P_3$ was added as an internal standard to the final concentration of 3.6 μM. The mixture was then injected on the HILIC-MS and $Ins(1,4,5)P_3$ was detected using selected ion monitoring mode. As expected, $[^{13}C_6]Ins(1,4,5)P_3$ and $[^{12}C_6]Ins(1,4,5)P_3$ co-eluted, and based on the ratio of $[^{13}C_6]Ins(1,4,5)P_3/[^{12}C_6]Ins(1,4,5)P_3$ ion counts, and on the standard curve, the consumption of $Ins(1,4,5)P_3$ could be quantified. Fig. 5(a) represents an example of the elution profiles of $[^{13}C_6]Ins(1,4,5)P_3$ *vs.* $[^{12}C_6]Ins(1,4,5)P_3$. The initial velocity of INPP5B using HILIC-MS was calculated to be 2.73 μmol mg^{-1} min^{-1}. (Fig. 5(b)). This initial velocity was 3.5-fold slower than that of calculated by real-time NMR based experiment previously in this paper. The observed slowing of the reaction could be attributed to differences in enzymatic reaction conditions, such as the solvent systems used in NMR *versus* HILIC-MS, potential degradation of the active enzyme during storage, changes in the substrate and enzyme concentrations to optimise the reaction for the particular method or variations in reaction monitoring—automated and continuous in NMR, compared to manual quenching followed by measurement in HILIC-MS.

Overall, in addition to its utility in NMR-based characterization, the labeled $[^{13}C_6]Ins(1,4,5)P_3$ also proved useful for monitoring the $Ins(1,4,5)P_3$ levels in complex biochemical samples using mass spectrometry.

Conclusions

$Ins(1,4,5)P_3$ is an important secondary messenger, yet the tools to probe its metabolism have limitations. Here, a semi-enzymatic route for the synthesis of $[^{13}C_6]Ins(1,4,5)P_3$, relying on the dephosphorylation of $[^{13}C_6]Ins(1,3,4,5,6)P_5$ catalyzed by the phosphatase MINPP1 was described. Using $[^{13}C_6]Ins(1,3,4,5,6)P_5$ as a starting material, $[^{13}C_6]Ins(1,4,5)P_3$ was obtained on milligram scale. We demonstrated the utility of this tool by testing it against two previously known $Ins(1,4,5)P_3$ metabolizing enzymes: the phosphatase INPP5B and the kinase IPMK. $^1H-^{13}C$ HMQC NMR spectroscopy enabled monitoring of the enzyme activities directly, without the need for radiolabeled substrates. In addition, the activity of a novel IPK enzyme from a microalga (*Kn*IPK2) was investigated. We discovered that unlike the orthologous plant enzyme *At*IPK2, *Kn*IPK2 is a 6-kinase and does not phosphorylate $Ins(1,4,5,6)P_4$ further *in vitro*. Interestingly, *Kn*IPK2 displayed ATP synthase activity towards $Ins(1,3,4,5,6)P_5$ and could dephosphorylate both positions 5 and 4/6 in the presence of ADP. Since the NMR chemical shifts can be directly correlated with the phosphorylation patterns, we predict that our tool holds potential to identify and characterize novel enzymes and metabolic pathways that use $Ins(1,4,5)P_3$ as a substrate. We envision using $[^{13}C_6]Ins(1,4,5)P_3$ as an internal standard for mass spectrometry-based metabolomics, and demonstrated that the HILIC-MS method presented here can assess $Ins(1,4,5)P_3$ turnover using this standard—providing a powerful approach to investigate the role of inositol phosphates (InsPs) *in vivo*. The synthesis of $[^{13}C_6]Ins(1,4,5)P_3$ and its dual

© 2025 The Author(s). Published by the Royal Society of Chemistry

RSC Chem. Biol., 2025, **6**, 1426–1436 | **1431**

application in NMR and MS also highlighted the complementarity of these two techniques—the former enables precise structural elucidation and the latter is favourable in applications where enhanced sensitivity for quantification is required.

Materials and methods

Instrumentation and chemicals

Non-labeled inositol phosphate standards for NMR measurements or HILIC-MS measurements were obtained from SiChem, Biomol, or Santa-Cruz. Used solvents were LC–MS grade and bought from VWR chemicals (Germany). The ammonia solution for adjusting the pH for HILIC-measurement was bought from Carl-Roth GmbH. The spin-filters for HILIC-MS workflow were bought from Merck Millipore Ltd. The Infinity-Lab Deactivator™ additive used in the LC–MS method for HILIC-measurements was bought from Agilent Technologies. For processing, analysis, and measurement of the NMR datasets, TopSpin 3.5 was used. All measurements were performed on a Bruker AV-III spectrometer (Bruker Biospin Theinstetten, Germany) equipped with a cryo-QCI probe. If not noted otherwise, chemicals were obtained from Sigma-Aldrich or Carl Roth Gmbh The LC–MS instrument was Agilent 1260 Infinity Binary LC coupled to an Agilent 6130 Single Quadrupole LC–MS System (Agilent, Waldbronn, Germany) with an electrospray ionization (ESI†) source. The high-resolution mass spectrometry was performed on Q Exactive Orbitrap Mass Spectrometers (Thermo Fisher Scientific Inc., Bremen, Germany) with a heated electrospray ionization (HESI†) source. The protein purifications were performed either on ÄKTA™ Purifier or NGC Quest 10 Chromatography System, Bio-Rad. The IMAC columns for purifications of proteins were obtained from GE Healthcare.

Synthesis of $[^{13}C_6]Ins(1,4,5)P_3$

$[^{13}C_6]Ins(1,3,4,5,6)P_5$ was synthesized according to the previously published protocol.[20] The MINPP1 phosphatase reaction using $[^{13}C_6]Ins(1,3,4,5,6)P_5$ as the substrate was carried out on 50 mL scale. 175 μM $[^{13}C_6]Ins(1,3,4,5,6)P_5$ was treated with 0.5 μM MINPP1 for 8 h at 37 °C. The conversion of $[^{13}C_6]Ins(1,3,4,5,6)P_5$ to $[^{13}C_6]Ins(1,4,5)P_3$ was followed by ^1H–^{13}C HMQC NMR spectroscopy. When the majority of the product formed was $[^{13}C_6]Ins(1,4,5)P_3$, the reaction was quenched by heating the reaction mixture at 95 °C for 5 min. 21 g of C18 reversed phase silica gel suspended in MeCN and sand was added on top in a fritted filter to form a C18 plug. Later the C18 plug was washed with 100 mL MeCN and 100 mL deionized water. The reaction mixture was passed through the C18 plug twice to ensure complete removal of protein. The flow-through was lyophilized and the protein-free crude reaction mixture was obtained as a white powder. The powdered reaction mixture was dissolved in 10 mL water. The dissolved flow-through was loaded onto an ion exchange column equilibrated with water at the flow-rate of 1 mL min⁻¹ using a flow performance liquid chromatography (FPLC) instrument. The elution of the bound InsPs was carried out using a 1–80% gradient of ammonium carbonate (pH 8)

followed by a final wash of 100% ammonium carbonate over 60 min at a flow-rate of 2 mL min⁻¹. The eluted fractions were collected and lyophilised and dissolved in 500 μL deuterated water and analysed by ^1H–^{13}C NMR spectroscopy. The fractions containing $[^{13}C_6]Ins(1,4,5)P_3$ were combined and lyophilised again to obtain 4.6 mg $[^{13}C_6]Ins(1,4,5)P_3$ as a white powder in the yield of 70%. (HRMS $[M - H]^{-1}$: 424.9727).

Protein expression and purification

INPP5B. The protocol for expression and purification of the 5-phosphatase INPP5B was modified from Trésaugues L et al.[18] In brief, INPP5B was expressed as a His-tagged protein in E. coli strain BL21 Rosetta 2 (DE3) using IPTG induction. Pre-cultures were inoculated in 50 mL terrific broth (TB) supplemented with 8 g L⁻¹ glycerol and 100 μg mL⁻¹ kanamycin and 34 μg mL⁻¹ chloramphenicol and incubated overnight at 37 °C. The pre-culture was inoculated 2 L TB with supplemented with 8 g L⁻¹ glycerol and 100 μg mL⁻¹ kanamycin, 34 μg mL⁻¹ chloramphenicol and were grown until the OD_{600} of 0.6–1.0 was achieved. The cultures were acclimatized at 18 °C for 1 h and later induced with 1 mM isopropyl 1-thio-β-D-galactopyranoside (IPTG). The induction was continued overnight. The cells were harvested by centrifuging at 5000 × g for 15 min at 4 °C. The cells were resuspended in buffer A (20 mM HEPES, pH 7.5, 500 mM NaCl, 10% glycerol, 10 mM imidazole, 1 mM DTT). Followed by this, the cells were chemically lysed by adding 1 spatula of lysozyme, 1 spatula of DNase, and protease inhibitors for 30 min. Later, the cells were lysed mechanically by microfluidizer at 15 000 psi with five iterations. The cell debris was removed by centrifuging the lysate at 20 000 × g. The supernatant was filtered through a 0.45 μm flask filter at 4 °C. The lysate was loaded onto IMAC column (5 mL) loaded with Nickel. The loaded column was washed with buffer A for 5 column volumes (CV). The elution was carried out by a gradient 1–100% buffer B (20 mM HEPES, 500 mM NaCl, 10% glycerol, 500 mM imidazole, 1 mM DTT, pH 7.5) over 20 min. The fractions were analysed by SDS-page and the fractions containing the protein were pooled together and dialysed against the dialysis buffer (20 mM HEPES, 300 mM NaCl, 10% glycerol, 1 mM DTT, pH 7.5) overnight at 4 °C.

IPMK. An overnight culture of the transformed E. coli BL21 cells in TB-Amp/Cam was diluted to a final OD_{600} of 0.05 in 800 mL TB supplemented with 0.07% (w/v) L-arabionose and grown for three hours at 37 °C. The temperature was switched to 18 °C and expression induced with 0.1 mM IPTG after half an hour. After 20 h expression the cells were pelleted by centrifugation (3000g, 10 min, 4 °C), washed with water and frozen at −80 °C. The pellet (10 g) was resuspended in 100 mL lysis buffer (20 mM Tris–HCl pH 7.4, 300 mM NaCl) supplemented with lysozyme, DNase I and protease inhibitor. After 30 min of incubation on ice the cells were lysed with a microfluidizer™ LM10 at 15 000 psi with five iterations. The cell debris was removed by centrifugation (25 000g, 25 min, 4 °C) and the supernatant lysate filtered (VWR vacuum filter, PES, 0.45 μm). The lysate was loaded onto an equilibrated 5 mL HiTrap IMAC HP column (GE Healthcare) at a flowrate of 1 mL min⁻¹,

© 2025 The Author(s). Published by the Royal Society of Chemistry

washed with 5 CV wash buffer (20 mM Tris–HCl pH 7.4, 300 mM NaCl, 20 mM imidazole) and eluted with a 0–100% gradient of elution buffer (20 mM Tris–HCl pH 7.4, 300 mM NaCl, 400 mM imidazole) in wash buffer over 10 CV. Fractions containing the protein were pooled and diluted with 190 mL anion exchange start buffer (20 mM Tris–HCl pH 8.2, 50 mM NaCl). The protein was loaded onto an equilibrated 5 mL HiTrap Q FF (GE Healthcare) column at a flowrate of 2 mL min^{-1}, washed with 3 CV of start buffer and eluted with a 0–100% gradient of elution buffer (20 mM Tris–HCl pH 8.2, 1 M NaCl) in start buffer over 10 CV. Fractions were concentrated by spin-filtration through 30 kDa cut-off filters to give 2.5 mL and loaded onto an equilibrated HiLoad 16/60 Superdex 200 pg column by injection. After elution with 20 mM Tris–HCl pH 7.4 in 150 mM NaCl at a flowrate of 1 mL min^{-1} fractions containing the protein were concentrated by spin-filtration through 10 kDa cut-off filters, adjusted to 16% glycerol and frozen at −80 °C.

KnIPK2. KnIPK2 was cloned RT-PCR form mRNA extracted for *Klebsormidium nitens* cultured cells. The coding sequence corresponds to A0A1Y1HXL1 available in UniProt database (https://www.uniprot.org/). *K. nitens* inositol polyphosphate multikinase 2 protein cDNA, was expressed in *E. coli* Rosetta II under the control of the T7 RNA polymerase promoter to enable synthesis of recombinant KnIPK2 protein with a His-tag at the N-terminus. Bacteria were grown at 37 °C in LB medium until OD_{600} was between 0.4 and 0.6. Protein production was induced by 0.5 mM IPTG for 3 h at 37 °C. Bacterial cells were then lysed in lysis buffer [20 mM Tris–HCl pH 7.4, 200 mM NaCl, 5 mM DTT, 1% (v/v) Triton X100, 0.5% (v/v) IGEPAL CA-630, Protease Inhibitor Cocktail (Roche)] and frozen in liquid nitrogen, then thawed and 0.1–1 mg mL^{-1} lysozyme, 21 µg^{-1} mg DNAse, and 7 µg mL^{-1} RNAse were added. The lysate was briefly sonicated and centrifuged at 20 000g for 30 min. Soluble proteins were passed through 0.22 µm filters before purification of His-tagged proteins by Ni^{2+} affinity chromatography using a His-TRAP™ column by FPLC on ÄKTA™ Purifier, according to the manufacturer's instructions (GE Healthcare). The column was washed with 4% imidazole before elution with a gradient up to 100%. After selection of fractions containing the protein of interest, these were pooled and dialyzed in 25 mM HEPES-KOH buffer pH 7.7, 1 mM ethylenedinitrilotetraacetic acid (EDTA) and 300 mM NaCl. Protein concentration was assessed by reading absorbance at 280 nm using a Nano-Drop™ spectrophotometer (ThermoScientific). His-KnIPK2 were stored at −80 °C in 20% glycerol without loss of activity.

Enzymatic assays

Phosphatase assays

NMR based activity test for INPP5B. The protocol was obtained from Trésaugues L *et al.* and modified for further use.[18] 200 µM of [$^{13}C_6$]Ins(1,4,5)P$_3$ was treated with 20 nM enzyme at 30 °C for 30 min in reaction buffer (HEPES pD 7.5, 300 mM NaCl, 250 µM MgCl$_2$, 1 mM DTT) in the total reaction volume of 100 µL. The reaction was heat quenched at 95 °C. The reaction was diluted 5-fold with deuterated water and transferred to NMR tubes for further measurements.

NMR based activity test for KnIPK2. KnIPK2 phosphatase activity was measured as follows: the phosphatase activity of KnIPK2 was measured using a deuterated system. The enzyme (20 nM) was incubated in the reaction buffer (50 mM Tris, 10 mM MgCl$_2$, 2 mM ADP) for 5 min. The reaction was started by adding [$^{13}C_6$]Ins(1,3,4,5,6)P$_3$ to the final concentration of 200 µM in a total volume of 100 µL. The reaction was heat quenched and diluted using 400 µL D$_2$O and analyzed using NMR as described in the section below.

Real-time monitoring of INPP5B activity using NMR. The protocol was obtained from Trésaugues L. *et al.* and modified for further use.[18] For real-time monitoring of the 5-phosphatase activity of INPP5B using NMR, 50 µM of the substrate [$^{13}C_6$]Ins(1,4,5)P$_3$ was treated with 10 nM enzyme at 37 °C in reaction buffer (HEPES pD 7.5, 300 mM NaCl, 250 µM MgCl$_2$, 1 mM DTT) in the total reaction volume of 500 µL. The reaction was run directly in the magnet and time points were recorded at the time intervals of 3.9 min until the reaction reached completion. The completion was confirmed by recording a ^{1}H–^{13}C HMQC NMR spectrum in the end.

Monitoring of INPP5B activity using HILIC-MS. The protocol was obtained from Trésaugues L. *et al.* and modified for further use.[18] 50 µM of Ins(1,4,5)P$_3$ was treated with 20 nM enzyme at 37 °C at time intervals of 10 min in reaction buffer (HEPES pH 7.5, 300 mM NaCl, 250 µM MgCl$_2$, 1 mM DTT) in the total reaction volume of 100 µL. The reaction was heat quenched at 95 °C at time intervals of 10 min. The reaction was diluted 4-fold with deionized water, filtered through 3 kDa filter, and subseqeuntly [$^{13}C_6$]Ins(1,4,5)P$_3$ was spiked in to the final concentration of 3.6 µM. Later on, the samples were subjected to HILIC-MS (mentioned below).

Kinase assays

IPMK kinase assay. The protocol was adapted from ref. 37 and modified as follows. The enzymatic activity of IPMK was measured using a deuterated system. 300 nM enzyme was incubated at 37 °C in the buffer 20 mM HEPES, 150 mM NaCl, and 2 mM MgCl$_2$, pH 7.5. The ATP concentration was 2 mM and the reaction was carried out in 500 µL reaction volume. The enzyme was acclimatized in the reaction conditions for 5 min. The reaction was started by adding [$^{13}C_6$]Ins(1,4,5)P$_3$ to a final concentration of 200 µM. After overnight incubation the reaction was heat quenched and analyzed using the NMR as described in NMR measurements.

KnIPK2 kinase assay. The kinase activity of KnIPK2 was measured using a deuterated system. KnIPK2 (20 nM) was incubated in the reaction buffer (50 mM Tris, 10 mM MgCl$_2$, 2 mM ATP) for 5 min. The reaction was started by adding [$^{13}C_6$]Ins(1,4,5)P$_3$ to a final concentration of 200 µM in a total volume of 100 µL. The reaction was heat quenched and diluted using 400 µL D$_2$O and analysed using NMR as described in the section below.

NMR measurements

For characterisation. The desired *in vitro* samples were dissolved or diluted in deuterated water (at least 500 µL) and

© 2025 The Author(s). Published by the Royal Society of Chemistry

RSC Chem. Biol., 2025, **6**, 1426–1436 | **1433**

transferred to a 5 mm NMR tube. For calculating the P1 pulse, the samples were manually locked, matched, and shimmed and the pulse recorded was used for the samples containing approximately the same salt concentrations. The operational magnetic field frequencies for ^{1}H, ^{13}C nuclei were 600 MHz, and 151 MHz, respectively. The pulse sequences for ^{1}H–^{13}C HMQC and ^{1}H–^{13}C HMQC-CLIP-COSY spectroscopy. The pulse sequences were derived from home-written programs. The parameters of measurements differed according to the sample, and the objective of the experiment. Typically for ^{1}H–^{13}C HMQC and ^{1}H–^{13}C HMQC-CLIP-COSY NMR spectroscopy 256 complex points were recorded when the characteristic triplet pattern of inositol species was desired otherwise 128 complex points or even less were recorded. The number of scans were kept at 64 or 1024 or 2048 when only the already confirmed species was to be detected. For ^{1}H–^{13}C HMQC-CLIP-COSY NMR spectroscopy 64 complex points were recorded and the number of scans was increased to 512 to improve the signal to noise ratio of the cross-peaks. All the samples were measured at 310 K. All the spectra were processed without digital water suppression with manual phase correction and automatic baseline correction.

For real-time monitoring experiments. The real-time experiments were also carried out in 5 mm NMR tubes and at 37 °C directly in the 600 MHz magnet. The pulse sequence was modified to record ^{1}H–^{13}C HMQC spectra with 64 scans, 1024 complex points in F3 (^{1}H), and 4 complex points in F2 (^{13}C) dimensions in restricted spectral width of 4.0159 ppm keeping the transmitter frequency offset at 75.087 ppm in the ^{13}C dimension for obtaining the time points for the INPP5B phosphatase reaction. Each ^{1}H–^{13}C HMQC NMR spectroscopy measurement was carried out for about 3.9 min. This was repeated 33 times to obtain 33 ^{1}H–^{13}C HMQC spectra one after the other. Later, the recorded spectra were stacked, and a pseudo plane was introduced to obtain an intensity against time curve.

HILIC-mass-spectrometry

Sample preparation. The diluted INPP5B treated samples were passed through 3 kDa spin filters to remove the protein from samples. [^{13}C$_6$]Ins(1,4,5)P$_3$ was spiked in and the filtrates were directly transferred to LC–MS vials and injected using autosampler.

HILIC-MS measurements. Analysis was performed on an Agilent 1260 Infinity Binary LC coupled to an Agilent 6130 Single Quadrupole LC–MS System (Agilent, Waldbronn, Germany) with an electrospray ionization (ESI†) source. The sample vials were maintained at room temperature in an autosampler. Hydrophilic interaction liquid chromatography was performed using a 2.0 × 150 mm, 5 μm HILICpak VG-50 2D column combined with a 2.0 × 10 mm, 5 μm HILICpak VG-50G 2A guard column (Shodex, Tokyo, Japan). Column oven was kept at 45 °C.[38] Mobile phase consisted of 10 mM NH$_4$HCO$_3$, 0.1% Agilent InfinityLab Deactivator Additive, pH 10.5 (buffer A) and 10% buffer A in MeCN with 0.1% Agilent InfinityLab Deactivator Additive. The injection volume was 2 μL. The elution started with a flow of 0.4 mL min^{-1} with 75% B held for 2.0 min and then decreased to 55% B between 2.0 min and 10.0 min, the flow was then reduced to

0.2 mL min^{-1} and B was further decreased to 2% between 10.0 min and 25.0 min. Between 25.0 min and 30.0 min B was held at 2%, then increased again to 75% between 30.0 min and 35.0 min. For equilibration of the column the flow was then set to 0.4 mL min^{-1} with 75% B for further 7 min. MS detection was performed using negative electrospray ionization. The ESI† source parameters were set as follows: spray voltage was set at 3 kV; drying gas flow at 12.0 L min^{-1}, nebulizer pressure at 55 psig; drying gas temperature at 300 °C. The peak width was set at 0.100 min and the cycle time was 0.60 s per cycle. The quadrupole was operated in selected ion monitoring (SIM) mode. Ins(1,4,5)P$_3$ was set as signal one with m/z 418.90 and [^{13}C$_6$]Ins(1,4,5)P$_3$ as signal two with m/z 425.00. For both signals a gain of 2.00, a dwell time of 290 ms and 50% cycle time were used. Peak detection, integration, and quantification were performed using OpenLab ChemStation Rev. C.01.07 SR3 (Agilent, Waldbronn, Germany).

High resolution mass spectra of Ins(1,4,5)P$_3$ and [^{13}C$_6$]-Ins(1,4,5)P$_3$ were obtained by using a Q Exactive Orbitrap Mass Spectrometers (Thermo Fisher Scientific Inc., Bremen, Germany) with a heated electrospray ionization (HESI) source. The Q Exactive was coupled to an UltiMate 3000 UHPLC system (Thermo Fisher Scientific Inc., Germering, Germany). The same chromatographic method as describe above was used.

MS detection was performed using full MS and negative electrospray ionization. The HESI source parameters were set as follows: spray voltage was set at 3.10 kV; sheath gas flow rate at 40 (arbitrary units); Aux gas flow rate at 15 (arbitrary units), Sweep gas flow rate at 1 (arbitrary units); capillary temperature at 275 °C, S-lens RF level at 100.0 and the Aux gas heater temperature at 350 °C. The needle was set in ring position C. The MS parameters were set as follows: the resolution was set to 70,00; the AGC target was set to 3e^6, the maximum IT was set to 200 ms and the scan range was set from 100 to 1500 m/z. No collision-induced dissociation was performed. Peak detection was performed using FreeStyle™ 1.8 SP2 Version 1.8.63.0 (Thermo Fisher Scientific Inc., Waltham, MA, USA).

Conflicts of interest

There are no conflicts to declare.

Data availability

The data supporting this article have been included in the Methods section, and as part of the ESI.†

Acknowledgements

1434 | *RSC Chem. Biol.*, 2025, **6**, 1426–1436

© 2025 The Author(s). Published by the Royal Society of Chemistry

Notes and references

1 V. Arige, L. E. Terry, L. E. Wagner, S. Malik, M. R. Baker and G. Fan, et al., Functional determination of calcium-binding sites required for the activation of inositol 1,4,5-trisphosphate receptors, Proc. Natl. Acad. Sci. U. S. A., 2022, 119(39), e2209267119.

2 B. C. Oh, Phosphoinositides and intracellular calcium signaling: novel insights into phosphoinositides and calcium coupling as negative regulators of cellular signaling, Exp. Mol. Med., 2023, 55(8), 1702–1712.

3 H. Wang and S. B. Shears, Structural features of human inositol phosphate multikinase rationalize its inositol phosphate kinase and phosphoinositide 3-kinase activities, J. Biol. Chem., 2017, 292(44), 18192–18202.

4 S. C. Chang, A. L. Miller, Y. Feng, S. R. Wente and P. W. Majerus, The human homolog of the rat inositol phosphate multikinase is an inositol 1,3,4,6-tetrakisphosphate 5-kinase, J. Biol. Chem., 2002, 277(46), 43836–43843.

5 M. Matzaris, C. J. O'Malley, A. Badger, C. J. Speed and P. I. Bird, Mitchell ChristinaA. Distinct Membrane and Cytosolic Forms of Inositol Polyphosphate 5-Phosphatase II, J. Biol. Chem., 1998, 273(14), 8256–8267.

6 D. Communi and C. Erneux, Identification of an active site cysteine residue in human type I Ins(1,4,5)P3 5-phosphatase by chemical modification and site-directed mutagenesis, Biochem. J., 1996, 320(Pt 1), 181–186.

7 Cloning, heterologous expression, and chromosomal localization of human inositol polyphosphate 1-phosphatase. [Internet]. [cited 2025 May 23]. Available from: https://www.pnas.org/doi/epdf/10.1073/pnas.90.12.5833.

8 R. C. Inhorn and P. W. Majerus, Inositol polyphosphate 1-phosphatase from calf brain. Purification and inhibition by Li$^+$, Ca^{2+}, and Mn^{2+}, J. Biol. Chem., 1987, 262(33), 15946–15952.

9 UniProt [Internet]. UniProt. [cited 2025 May 23]. Available from: https://www.uniprot.org/uniprotkb/Q96PE3/entry.

10 K. Pattni and G. Banting, Ins(1,4,5)P3 metabolism and the family of IP3-3Kinases, Cell Signalling, 2004, 16(6), 643–654.

11 S. Kim, R. Bhandari, C. A. Brearley and A. Saiardi, The inositol phosphate signalling network in physiology and disease, Trends Biochem. Sci., 2024, 49(11), 969–985.

12 C. M. Dovey, J. Diep, B. P. Clarke, A. T. Hale, D. E. McNamara and H. Guo, et al., MLKL requires the inositol phosphate code to execute necroptosis, Mol. Cell, 2018, 70(5), 936–948.

13 E. Ucuncu, K. Rajamani, M. S. C. Wilson, D. Medina-Cano, N. Altin and P. David, et al., MINPP1 prevents intracellular accumulation of the chelator inositol hexakisphosphate and is mutated in Pontocerebellar Hypoplasia, Nat. Commun., 2020, 11(1), 6087.

14 B. Appelhof, M. Wagner, J. Hoefele, A. Heinze, T. Roser and M. Koch-Hogrebe, et al., Pontocerebellar hypoplasia due to bi-allelic variants in MINPP1, Eu.r J. Hum. Genet., 2021, 29(3), 411–421.

15 H. Whitfield, A. M. Hemmings, S. J. Mills, K. Baker, G. White and S. Rushworth, et al., Allosteric Site on SHIP2 Identified Through Fluorescent Ligand Screening and Crystallography: A Potential New Target for Intervention, J. Med. Chem., 2021, 64(7), 3813–3826.

16 S. Dragon, R. Hille, R. Götz and R. Baumann, Adenosine 3′:5′-cyclic monophosphate (cAMP)-inducible pyrimidine 5′-nucleotidase and pyrimidine nucleotide metabolism of chick embryonic erythrocytes, Blood, 1998, 91(8), 3052–3058.

17 F. M. Gribble, G. Loussouarn, S. J. Tucker, C. Zhao, C. G. Nichols and F. M. Ashcroft, A Novel Method for Measurement of Submembrane ATP Concentration, J. Biol. Chem., 2000, 275(39), 30046–30049.

18 L. Trésaugues, C. Silvander, S. Flodin, M. Welin, T. Nyman and S. Gräslund, et al., Structural basis for phosphoinositide substrate recognition, catalysis, and membrane interactions in human inositol polyphosphate 5-phosphatases, Structure, 2014, 22(5), 744–755.

19 H. L. Whitfield, R. F. Rodriguez, M. L. Shipton, A. W. H. Li, A. M. Riley and B. V. L. Potter, et al., Crystal Structure and Enzymology of Solanum tuberosum Inositol Tris/Tetrakisphosphate Kinase 1 (StITPK1), Biochemistry, 2024, 63(1), 42–52.

20 R. K. Harmel, R. Puschmann, M. N. Trung, A. Saiardi, P. Schmieder and D. Fiedler, Harnessing 13C-labeled myo-inositol to interrogate inositol phosphate messengers by NMR, Chem. Sci., 2019, 10(20), 5267–5274.

21 T. Aguirre, G. L. Dornan, S. Hostachy, M. Neuenschwander, C. Seyffarth and V. Haucke, et al., An unconventional gatekeeper mutation sensitizes inositol hexakisphosphate kinases to an allosteric inhibitor, eLife, 2023, 12, RP88982.

22 M. Nguyen Trung, S. Kieninger, Z. Fandi, D. Qiu, G. Liu and N. K. Mehendale, et al., Stable Isotopomers of myo-Inositol Uncover a Complex MINPP1-Dependent Inositol Phosphate Network, ACS Cent. Sci., 2022, 8(12), 1683–1694.

23 G. Liu, E. Riemer, R. Schneider, D. Cabuzu, O. Bonny and C. A. Wagner, et al., The phytase RipBL1 enables the assignment of a specific inositol phosphate isomer as a structural component of human kidney stones, RSC Chem Biol, 2023, 4(4), 300–309.

24 P. Li and M. Lämmerhofer, Generation of 13C-Labeled Inositol and Inositol Phosphates by Stable Isotope Labeling Cell Culture for Quantitative Metabolomics, Anal. Chem., 2022, 94(44), 15332–15340.

25 A. C. Schmid, H. M. Wise, C. A. Mitchell, R. Nussbaum and R. Woscholski, Type II phosphoinositide 5-phosphatases have unique sensitivities towards fatty acid composition and head group phosphorylation, FEBS Lett., 2004, 576(1–2), 9–13.

26 T. S. Ross, A. B. Jefferson, C. A. Mitchell and P. W. Majerus, Cloning and expression of human 75-kDa inositol

© 2025 The Author(s). Published by the Royal Society of Chemistry

RSC Chem. Biol., 2025, 6, 1426–1436 | 1435

polyphosphate-5-phosphatase, *J. Biol. Chem.*, 1991, **266**(30), 20283–20289.

27 A. B. Jefferson and P. W. Majerus, Properties of Type II Inositol Polyphosphate 5-Phosphatase (*), *J. Biol. Chem.*, 1995, **270**(16), 9370–9377.

28 S. J. Mills, C. Silvander, G. Cozier, L. Trésaugues, P. Nordlund and B. V. L. Potter, Crystal Structures of Type-II Inositol Polyphosphate 5-Phosphatase INPP5B with Synthetic Inositol Polyphosphate Surrogates Reveal New Mechanistic Insights for the Inositol 5-Phosphatase Family, *Biochemistry*, 2016, **55**(9), 1384–1397.

29 H. Wang and S. B. Shears, Structural features of human inositol phosphate multikinase rationalize its inositol phosphate kinase and phosphoinositide 3-kinase activities, *J. Biol. Chem.*, 2017, **292**(44), 18192–18202.

30 A. R. Odom, A. Stahlberg, S. R. Wente and J. D. York, A Role for Nuclear Inositol 1,4,5-Trisphosphate Kinase in Transcriptional Control, *Science*, 2000, **287**(5460), 2026–2029.

31 P. Chatelain, C. Blanchard, J. Astier, A. Klinguer, D. Wendehenne and S. Jeandroz, *et al.*, Reliable reference genes and abiotic stress marker genes in Klebsormidium nitens, *Sci. Rep.*, 2022, **12**(1), 18988.

32 K. Hori, F. Maruyama, T. Fujisawa, T. Togashi, N. Yamamoto and M. Seo, *et al.*, Klebsormidium flaccidum genome reveals primary factors for plant terrestrial adaptation, *Nat. Commun.*, 2014, **5**(1), 3978.

33 J. Stevenson-Paulik, A. R. Odom and J. D. York, Molecular and Biochemical Characterization of Two Plant Inositol Polyphosphate 6-/3-/5-Kinases, *J. Biol. Chem.*, 2002, **277**(45), 42711–42718.

34 J. Xu, C. A. Brearley, W. H. Lin, Y. Wang, R. Ye and B. Mueller-Roeber, *et al.*, A Role of Arabidopsis Inositol Polyphosphate Kinase, AtIPK2α, in Pollen Germination and Root Growth, *Plant Physiol.*, 2005, **137**(1), 94–103.

35 K. Ritter, N. Jork, A. S. Unmüßig, M. Köhn and H. J. Jessen, Assigning the Absolute Configuration of Inositol Poly- and Pyrophosphates by NMR Using a Single Chiral Solvating Agent, *Biomolecules*, 2023, **13**(7), 1150.

36 D. Qiu, M. S. Wilson, V. B. Eisenbeis, R. K. Harmel, E. Riemer and T. M. Haas, *et al.*, Analysis of inositol phosphate metabolism by capillary electrophoresis electrospray ionization mass spectrometry, *Nat. Commun.*, 2020, **11**(1), 6035.

37 I. Cestari, A. Anupama and K. Stuart, Inositol polyphosphate multikinase regulation of Trypanosoma brucei life stage development, *Mol. Biol. Cell*, 2018, **29**(9), 1137–1152.

38 M. Ito, N. Fujii, C. Wittwer, A. Sasaki, M. Tanaka and T. Bittner, *et al.*, Hydrophilic interaction liquid chromatography–tandem mass spectrometry for the quantitative analysis of mammalian-derived inositol poly/pyrophosphates, *J. Chromatogr. A*, 2018, **1573**, 87–97.